INTEGRATED USE OF SURFACE-GEOPHYSICAL METHODS TO INDICATE SUBSURFACE FRACTURES AT TIBBETTS ROAD, BARRINGTON, NEW HAMPSHIRE

By D.A. Lieblich, F.P. Haeni, and Rowland E. Cromwell

U.S. GEOLOGICAL SURVEY

Water-Resources Investigations Report 92-4012

Prepared in cooperation with the

U.S. ENVIRONMENTAL PROTECTION AGENCY

Hartford, Connecticut

1992

U.S. DEPARTMENT OF THE INTERIOR

MANUEL LUJAN, JR., Secretary

U.S. GEOLOGICAL SURVEY

Dallas L. Peck, Director

For additional information write to:

Chief, Connecticut District
U.S. Geological Survey
450 Main Street, Room 525
Hartford, CT 06103

Copies of this report can be purchased from:

U.S. Geological Survey
Books and Open-File Reports Section
Federal Center, Box 25425
Denver, CO 80225

CONTENTS

ILLUSTRATIONS

ILLUSTRATIONS (continued)

CONVERSION FACTORS

Multiply	by	To obtain
meter (m)	3.281	foot
kilometer (km)	0.6214	mile
kilometer per hour (km/hr)	0.6214	mile per hour
kilometer per second (km/s)	3,281	foot per second
meter per nanoseconds (m/ns)	3.281	foot per nanosecond
millisiemen per meter (mS/m)	0.305	millisiemen per foot
ohm-meter (ohm-m)	3.281	ohm-foot

INTEGRATED USE OF SURFACE-GEOPHYSICAL METHODS TO INDICATE SUBSURFACE FRACTURES AT TIBBETTS ROAD, BARRINGTON, NEW HAMPSHIRE

by D.A. Lieblich, F.P. Haeni, and Rowland E. Cromwell

ABSTRACT

Four surface-geophysical methods were used to indicate the presence and estimate the orientations of subsurface fractures at a site on Tibbetts Road, near Barrington, New Hampshire. The methods used were ground-probing radar, inductive terrain conductivity, direct-current resistivity, and seismic refraction.

Three of the four geophysical data sets contain anomalies that are interpreted as representing subsurface fracturing. Interpretation of the individual data sets yields some conflicting results; however, an integrated interpretation indicates one fracture set oriented east--close to the orientations found in previous studies. Unmigrated ground-probing radar data show multiple, coherent events that dip steeply on the time section and can be interpreted as representing fractures. After migration, however, these events disappear, indicating that they are artifacts of the scattering process. Multiple, coherent events that are subhorizontal are present on the migrated section. One event is the top of bedrock and another is system noise. Other events could include a multiple reflection of the bedrock surface, foliation, fracturing, or a combination of these. No anomalies caused by fractures were interpreted from the limited inductive terrain-conductivity data collected at this site. Interpretation of direct-current resistivity data indicates two different sets of fractures in the bedrock that are oriented east and north-northwest. A third set of fractures oriented northeast also could be present. A fracture set that trends east is interpreted from the seismic-refraction data.

INTRODUCTION

Bedrock with normally low, primary permeability may be capable of substantial fluid transport if it is fractured. Fractures can act as conduits through the bedrock, and, because their orientations are not usually random, they may introduce a significant anisotropy to the subsurface flow pattern. Surface-geophysical methods can indicate the orientations of subsurface fractures and thereby provide data that may also indicate a preferred flow direction.

A study was undertaken by the U.S. Geological Survey (USGS), in cooperation with the U.S. Environmental Protection Agency (USEPA), to determine whether surface-geophysical methods could indicate the presence and estimate the orientations of subsurface fractures at a site on Tibbetts Road, near Barrington, New Hampshire (fig. 1). The study site is near a USEPA Superfund site where hazardous fluids have been found in the overburden and bedrock. Regional geologic data and local hydraulic data indicate that the bedrock is fractured. Characterization of the fluid transport properties of the subsurface at this site is of primary importance in assessing the occurrence and movement of contamination, as well as in developing methods to limit or eliminate contamination.

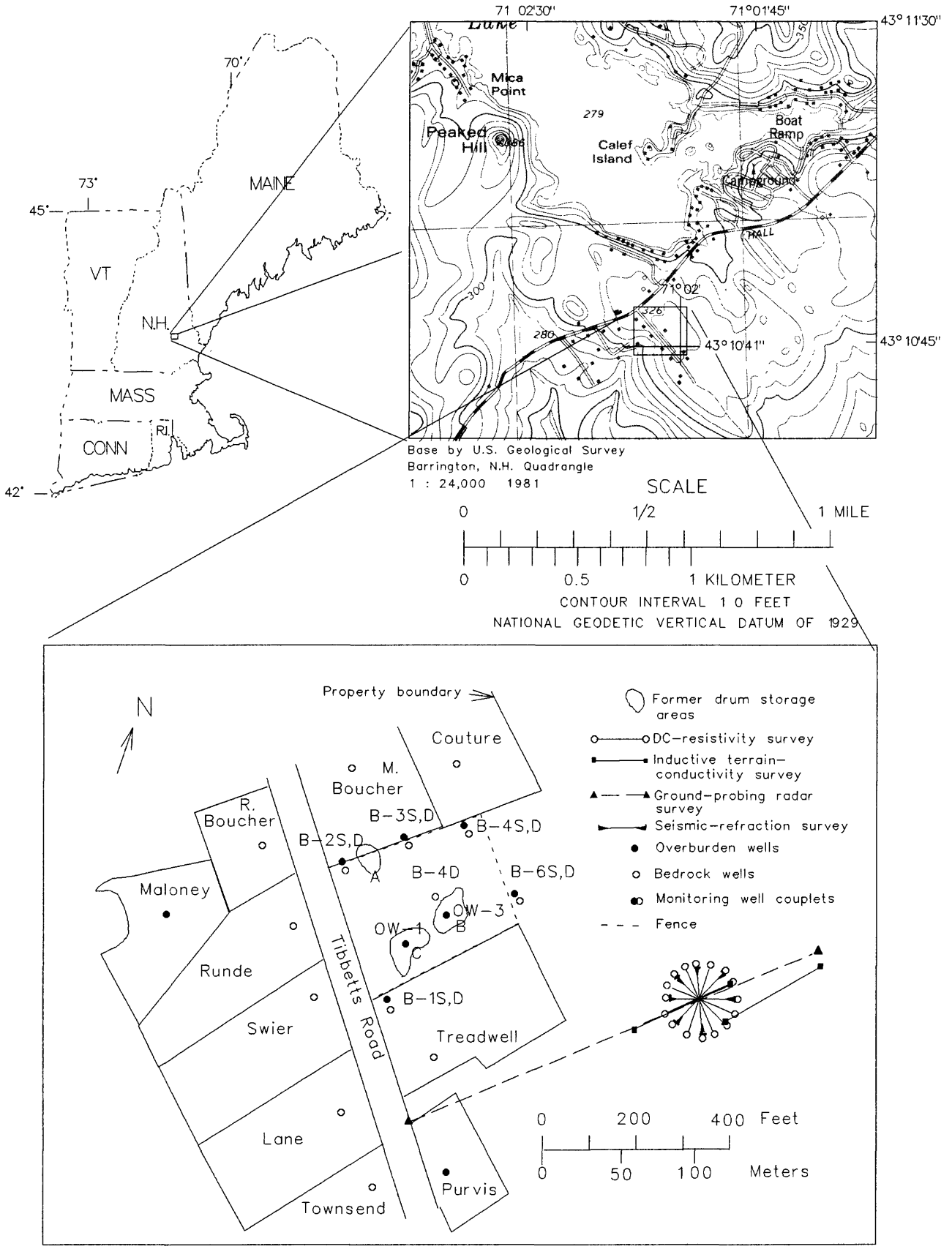

Figure 1.--Location of study area and geophysical surveys.

Purpose and Scope

This report (1) presents the results of a study to determine if surface-geophysical methods could be used to indicate the presence and estimate the orientations of subsurface fractures and (or) fracture zones, at a site on Tibbetts Road, near Barrington, New Hampshire; and (2) provides information (derived from the individual and integrated interpretation of the geophysical-data sets) useful for site characterization and remediation.

A review of previous studies, which provides a description of the study area, is followed by a brief summary of each surface-geophysical method used in this study. A general description of the approach to geophysical investigations at this site follows. For each method, details of the data acquisition precede the data presentation.

A thorough assessment of the problems associated with the surface-geophysical methods used for subsurface fracture detection is beyond the scope of this report. This report is restricted to a description of the application of relatively standard and readily available surface-geophysical methods.

Description of the Study Area and Previous Investigations

The study area is located in the glaciated northeastern United States 4.6 km south of the town of Barrington, New Hampshire. The study area is underlain by fractured crystalline bedrock with a till cover. A private residence on Tibbetts Road is reported to be the source of contamination to local residential water wells. A fence has been placed around the contaminated area (fig. 1).

The study area has been described in the following four reports: (1) a report by BCI Geonetics (1984) on bedrock fracture analysis; (2) a report by the Hydrological Investigation Unit of the New Hampshire Water Supply and Pollution Control Commission (NHWSPCC) (1985) that includes a local geologic overview, as well as interpretations of data collected by seismic refraction, direct-current (DC) resistivity, and electromagnetic (EM) surveys; (3) a report by Posten and others (1986) that provides hydrologic analysis of bedrock flow patterns, based on straddle packer aquifer tests and borehole logs for bedrock wells; and (4) a report by McCormick (1989) that provides site details from an analysis of historical aerial photography.

Geologic Data

Shallow wells were drilled into overburden and deeper wells were drilled into bedrock within and near the fenced area to characterize the hydrology of the overburden and bedrock. Borehole logs from these wells provide the most detailed information on the lithology and thickness of subsurface layers. These logs show a progression from sandy till in the near surface, to a transitional sandy-silty till, to a dense silty till overlying a monzonitic bedrock (New Hampshire Water Supply and Pollution Control Committee, 1985). The thickness of the overburden ranges from 3 to 21 m. Seismic-refraction lines corroborate the local bedrock depth obtained from borehole information and extend it over a larger region (New Hampshire Water Supply and Pollution Control Committee, 1985). Bedrock wells, which were drilled about 46 m into the bedrock, encountered many fracture zones.

Fracture data are available from one well, B6-D, where coring was done. The unoriented core shows that steeply dipping fractures (74° to 80° (degrees)) and subhorizontal fractures are present. A subhorizontal foliation, which may control the subhorizontal fractures, also is present in the core.

The BCI Geonetics (1984) report provides important data on the orientation, density, and characteristics of fractures from four outcrop stations, located 3 to 6 km from the site. The results show that fractures striking northwest (NW) are the most numerous, are open, and are continuous for tens of meters. The next most pervasive fracture set strikes north-northeast (NNE). It contains individual fractures that are continuous for meters and are sometimes filled with quartz. The data showing measured outcrop fracture strike frequency as a function of azimuth are summarized in figure 2 (BCI Geonetics, 1984). Fracture dips were not noted in the report, but they are assumed to be steep. Three other sets of fracture orientations were noted in the report as minor but of possible local importance; their orientations are east-northeast (ENE), north-northwest (NNW) and north.

The BCI Geonetics (1984) report includes a photolineament analysis of the study area. The most prominent photolineaments are oriented NW and were noted as prime candidates for fractured bedrock aquifers. Other lineaments are oriented ENE and NNE. These lineaments were not identified close to the site, but the possibility of their occurrence cannot be ruled out.

Hydrologic Data

Straddle packer aquifer tests were conducted by Posten and others (1986) at two depth intervals in each of two deep bedrock wells. The purpose of these tests was to assess migration of contaminants in the bedrock by defining the orientations and transmissivities of hydraulic connections between each of the 2 pumped wells and 21 monitoring wells. The results in one well show hydraulic connections to the monitoring wells at angles of 120°, 165°, and 237° from true north. These connections are continuous across both packed-off intervals (33.5 to 39.6 m and 42.7 to 51.8 m). The other well shows hydraulic connections to the monitoring wells at angles of 16°, 120°, and 184° from true north. Only the 120°- and 184°-connections were continuous across both packed-off intervals (21.3 to 27.4 m and 54.9 to 61.0 m). It was concluded that "fracture permeability within and adjacent to the Tibbetts Road site is preferentially oriented along NE-SW and NW-SE axes." It should be noted that the accuracy with which the orientation of a hydraulic connection can be determined, using these data, depends on the azimuthal density of well coverage; the density varies at this site (Posten and others, 1986, figs. 3 to 6).

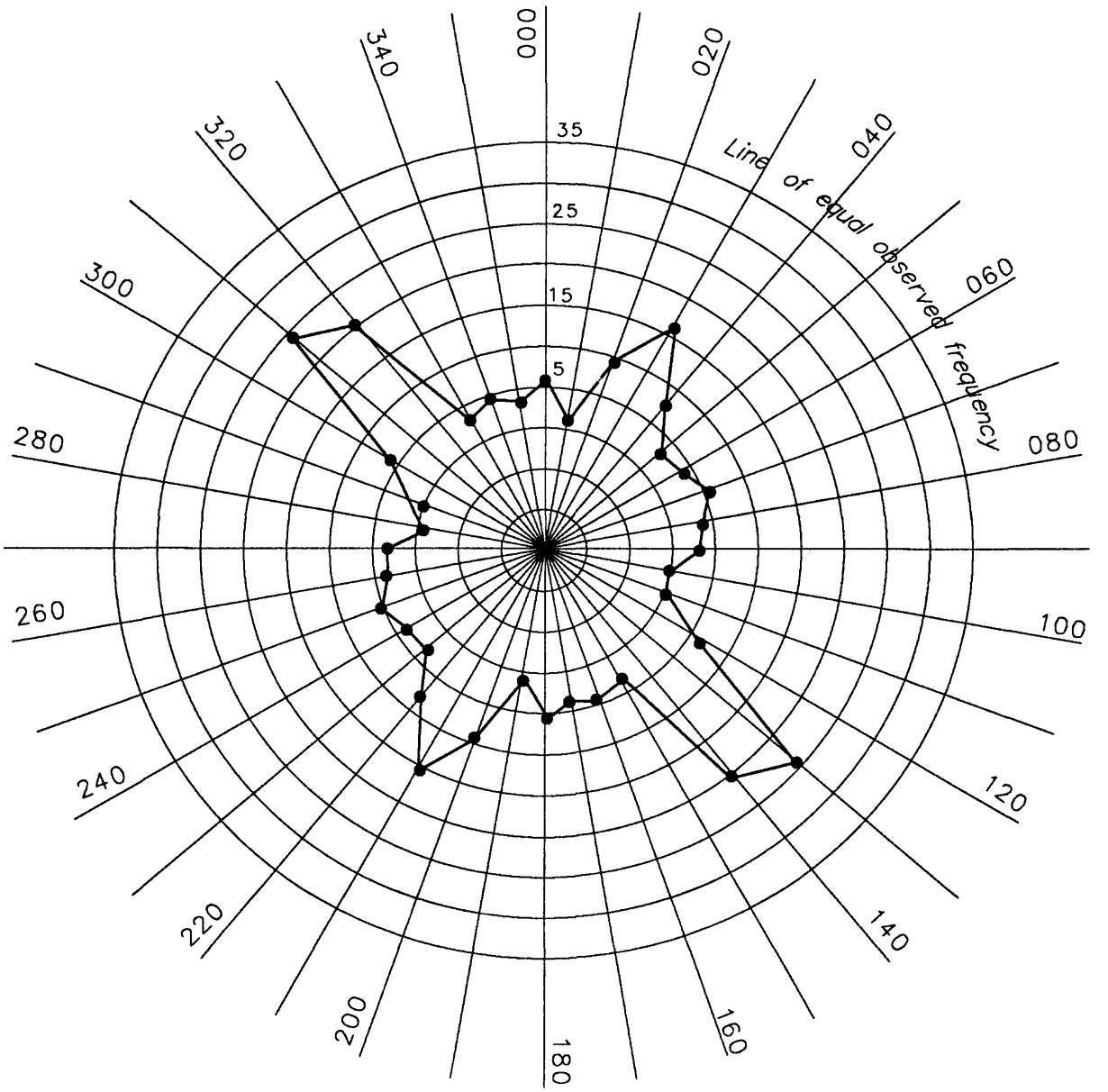

EXPLANATION

000 = Degrees from magnetic north

● Fracture strike frequency measured in outcrop

Figure 2.--Strike frequency of measured outcrop fractures as a function of azimuth. (Modified from BCI Geonetics, 1984, fig. 3.)

PRINCIPLES OF SURFACE-GEOPHYSICAL METHODS

A brief review of the surface-geophysical methods used in this study is given below. These methods are ground-probing radar (GPR), inductive terrain conductivity, DC resistivity, and seismic refraction. The order of discussion is from the fastest to the slowest method in terms of data-collection time in the field. Although the order is not intended to indicate how a field program should be designed, it does represent one way of designing such a program.

Ground-Probing Radar

GPR uses transmitter and receiver antennae, which may be the same unit, to generate and detect subsurface EM waves. Measurable signals can be obtained when the EM wave encounters changes to any individual or combination of the following physical properties: conductivity, dielectric permittivity, and magnetic permeability. The advantage of GPR for fracture detection is that the conductivity and dielectric permittivity usually change significantly in a fluid saturated fracture or fracture zone compared to the properties in the host rock. The image of a fracture on a radar section can range from a sublinear coherent event[1/] to a diffraction hyperbola with a "ringy" appearance. Discontinuous layers or foliation, as well as localized, small scatters, can also produce sublinear coherent events and diffraction hyperbolas.

In previous investigations, at other sites, Ulriksen (1982) obtained reflections from individual fractures or fracture zones in granodiorite. Imse and Levine (1985) obtained strong scattering responses from steeply dipping fractures in carbonate rocks in northern New York. Olsson and others (1988) obtained reflections in crystalline rocks from steeply dipping individual fractures with a borehole radar unit.

In addition to the possibility of detecting signals from individual fractures or fracture zones directly, GPR can also be used to map the depth to bedrock and changes in the overburden. These data can be used to reduce the ambiguity in seismic-refraction interpretations. In shallow studies, the bedrock-overburden interface usually represents a significant contrast in elastic and electric properties thus generating a radar reflection as well as refracted and reflected seismic waves. If radar-velocity information is available or is measured, the radar image can be used to determine the thickness of material above the interface.

Inductive Terrain Conductivity

Two coils, a transmitter and a receiver, are used in the inductive terrain-conductivity method. Alternating current flowing in the transmitter coil causes a primary magnetic field. This magnetic field induces eddy currents in the subsurface, which, in turn, cause a secondary magnetic field. The receiver coil measures the ratio of the secondary magnetic field to the primary magnetic field. In general, the EM field responds to changes in conductivity, dielectric permittivity, and magnetic permeability.

1/ As used in this report, an event is "a lineup on a number of traces which indicates the arrival of new seismic energy...May indicate a reflection, refraction, diffraction, or other type of wavefront."

Changes in the magnetic permeabilities of rocks are generally negligible, and, because of the low frequency of the signal used, displacement currents caused by the dielectric properties of the medium are also negligible. Measurements are, therefore, sensitive to changes in the conductivity of the subsurface.

A mobile source is used in the inductive terrain-conductivity method, and allows dipping fractures of any strike to be detected. In addition, operation under the low-induction-number assumption (McNeill, 1980a) permits the depth of penetration to be varied by changing the operating frequency and the intercoil spacing. Orienting the two coils either vertically or horizontally causes preferential sensitivity in the instrument response to subsurface structures with different orientations. Sensitivity to vertical or near vertical conductors, such as fluid-filled fractures, is obtained by orienting the coils horizontally (the vertical dipole mode) (McNeill, 1980b, fig. 6). In this orientation, the image of a subsurface vertical conductor is a symmetric waveform centered over the conductor and with a peak to peak distance equal to two coil spacings. If this method is used in areas with conductive overburden, small increases in the thickness of the conductive overburden can cause anomalies similar in size and shape to those caused by vertical conductors (Villegas-Garcia and West, 1983).

Successful use of the method for fracture detection, using the coils in the vertical dipole mode, has been demonstrated by Palacky and others (1981) and by van Lissa and others (1987) in fractured granitic rocks where faults and fracture zones were identified on aerial photographs. In addition, a recent study in carbonate rocks by Yager and Kappel (1988) has demonstrated the use of an inductive terrain-conductivity instrument (Geonics EM-34[2/]) for high-angle fracture detection in sedimentary rocks.

Direct-Current Resistivity

The DC-resistivity method uses either a DC current or an alternating current with a frequency commonly below 10 Hz (Hertz). The method is commonly applied by sending current into the ground through two electrodes and measuring the potential difference (voltage) at two other electrodes. The apparent resistivity (resistivity of a homogeneous, isotropic volume of earth) is estimated for a specific electrode spacing and geometry. Ideally, the apparent resistivity is independent of measured voltage and input current; however, the presence of ambient noise often causes deviations. The DC-resistivity method measures the apparent resistivity of a volume of rock, which is usually large compared to the scale of and the spacing between individual fractures or fracture zones. This may require the rock to be treated as an anisotropic medium and increases the scope and complexity of the interpretation.

The DC-resistivity method is especially useful in differentiating rock units with varying resistivities, and its depth of penetration is controlled primarily by the spacing of the current electrodes. Near surface and three-dimensional effects are inherent in real data, and normal interpretive methods do not account for them. The most common application of the DC-resistivity method for the detection of fractures in rock is to identify and correlate low-resistivity zones in a grid of resistivity traverses.

[2/] Use of trade names is for identification purposes only and does not constitute endorsement by the U.S. Geological Survey.

Rotation of linear arrays (either Wenner or Schlumberger) has also been used to identify the presence of small but pervasive fractures that cause an anisotropic bulk resistivity. It should be noted that the interpretation of azimuthal resistivity data is not intuitive--for a single zone of oriented subvertical fractures, the apparent resistivity maximum corresponds to the orientation of the fractures with the apparent resistivity minimum oriented orthogonally. However, the orientation of the fractures is also the true resistivity minimum. This phenomenon is known as the "paradox of anisotropy" (Keller and Frischknecht, 1966, p. 103). Azimuthal resistivity measurements over a layered subsurface can also produce an anisotropic bulk resistivity, if the layering is not parallel to the surface on which measurements are made.

Successful detection of fractures using azimuthal DC-resistivity surveys has been demonstrated in the following studies: Risk (1975) in volcanic rocks; McDowell (1979) in granitic rocks overlain by fluvial sediments; Palacky and others (1981) in fractured granitic rocks associated with faults and fracture zones identified on aerial photographs; Soonawala and Dence (1981) in granitic rocks; Taylor (1982) in carbonates overlain by till; Mallik and others (1983) in granites, amphibolites, and metabasic rocks; Leonard-Mayer (1984a, 1984b) in carbonate rocks overlain by up to 2 m of soil or glacial deposits; Ogden and Eddy (1984) in carbonate rocks; Taylor (1984) in carbonates overlain by till; and Taylor and Fleming (1988) in gabbro, basalt, dolomite, and till.

Seismic Refraction

The seismic-refraction method uses an impulsive source to generate elastic waves that propagate through the subsurface. In standard applications, a compressional wave (p-wave) is used, although shear waves (s-waves) may also be used. The critically refracted (head) wave, either p or s, is detected as a strong change in particle velocity (or acceleration) at geophones on the surface when there is a seismic velocity increase at depth. For constant velocity layers, there is a linear change in arrival time as a function of detector distance. This change can be used to obtain the velocity at which the head wave travels through the medium. For a homogeneous, isotropic medium, the velocity is a function of the density, compressibility, and shear modulus of the medium.

The effects of single fractures or small isolated fracture zones are unlikely to be seen in p-wave refraction surveys of any kind because the velocity and (or) attenuation changes caused by these objects are normally too small to be detected. Azimuthal refraction methods can detect an anisotropic distribution of pervasive fractures in the bulk rock. For a single subvertical fracture set, a velocity maximum occurs along the strike direction, and a velocity minimum occurs orthogonal to the strike direction. Velocity and (or) thickness inhomogeneities in the material overlying the reflector can also generate an anisotropic azimuthal velocity function.

P-wave refraction experiments that have successfully detected fractures include: Bamford and Nunn (1979) and Crampin and others (1980) in carbonate rocks; Park and Simmons (1982) in granites, quartz syenites, and volcanic rocks with glacial overburden; and Imse and Levine (1985) in carbonate rocks with glacial overburden.

Fractures represent discontinuities in an otherwise continuous and, in the simplest case, homogeneous body of rock. If fractures are inhomogeneously and (or) anisotropically distributed throughout a rock body, the physical properties of the bulk rock may require mathematical formulations that consider the rock body to be either inhomogeneous, anisotropic, or both. These topics remain at the forefront of geophysical research (Frazer, 1990; Wait, 1990). Existing, simple theories can be used to interpret geophysical methods that are sensitive to rock physical properties at wavelengths comparable to the size of individual fractures or fractures zones.

Despite the developmental state of theoretical ideas, observational data from experimental and field studies have been, and continue to be, successfully collected (see individual methods in previous section). The basic conclusion that can be drawn from most of these investigations is that the change in the bulk physical properties of the rock caused by fracturing is generally small. Therefore, for each method, great care must be exercised during survey design and data collection to minimize all effects that could interfere with and (or) mask the effects of fractures.

Interferences from various natural or cultural sources may mask or seriously degrade the data and decrease the possibility of detecting a clear fracture response. Although filtering techniques can be applied, they are seldom perfect and may be inappropriate for weak signals, emphasizing the importance of obtaining as many independent data sets as possible. Constrained interpretation of these data sets through either a simple, manual cross correlation (integration), as is done here, or through a complex, integrated inversion technique should improve confidence in the results and perhaps improve resolution over what could be obtained by use of a single method.

The design of each surface-geophysical survey considered all available information on strength, spatial orientation, size, and shape of the expected physical property anomaly, as well as the distance from the source of the anomaly to the detectors. Residual contaminants are assumed to have a negligible effect on the bulk physical properties, as measured by the methods used in this study, because of their very small concentrations.

Optimal survey design considered not only the detection of individual geophysical anomalies, but also the interpretation of different geophysical data. This additional consideration arose because of the desire to integrate the interpretational results of the different methods. Optimal survey design was implemented by requiring that at least some of the data points from the different survey grids coincided. Ultimately, a compromise was struck between the economically defined grids, the optimal survey design, and site logistics.

Data were collected in a clearing in the woods, 198 m southeast of the fenced contamination area on Tibbetts Road. A single GPR line oriented northeast and four radiating seismic-refraction lines at azimuths of north, northeast, east, and northwest were collected (fig. 1). One line of inductive terrain-conductivity data, oriented NNE and eight DC-resistivity lines spaced 22.5° apart in azimuth, starting at north, were also collected.

GPR, inductive terrain-conductivity, DC-resistivity, and compressional-wave seismic-refraction data sets collected at Tibbetts Road near Barrington, New Hampshire are presented in this section. Details of data acquisition for each method are presented first; this is followed by observations and interpretations for each data set.

Ground-Probing Radar

A radar unit manufactured by Geophysical Survey Systems Inc. (GSSI) was used in the survey. A bistatic antenna configuration operating at a center frequency of 80 MHz (megahertz) was used. The antennae were towed about 30 m behind a vehicle moving at approximately 4.8 km/hr. A scan rate of 25.6 scans per second and a time scale of 900 ns (nanoseconds) was used. The range gain was adjusted in the field and recorded to allow for a more appropriate adjustment during processing. The records were marked for every 9.1 m of ground covered, and the two-way travel time was printed on the records. Because the area was heavily wooded, only one GPR line was run along a logging road oriented from NE to SW. The radar section shown in figure 3 has been corrected by horizontally stretching and compressing the data between marks to eliminate the effect of the varying truck speed.

Interpretive processing was performed using GSSI's RADAN processing package; "attribute sections" showing the different attributes of the Hilbert Transform were produced. These sections were found to be helpful in correlating events laterally along a traverse. In addition, the record was migrated using a velocity of 0.057 m/ns (fig. 3b) determined from scatterers that appear in the section. It should be noted that the velocity used to migrate the section does not, in general, represent the medium velocity; the migration velocity is equivalent to the seismic stacking velocity. Concave upward events in the migrated section appear at the locus of marks in the unmigrated section; these are artifacts caused by the migration process, which smears the marks out across the section.

Trees and branches were thought to be the dominant contribution to the noise, because the 80 MHz antennae were not shielded. Analysis of moveouts of the recorded events indicated that trees did not cause the noise on this radar section.

Observations and Interpretations

1. Observation: Subparallel events dip approximately 45° (relative to the X axis) towards the southwest and others dip approximately 45° towards the northeast (1 on fig. 3a). These events are not present on the migrated section (fig. 3b).

   Interpretation: Events that might be interpreted as NE and SW dipping fracture sets on the unmigrated section are seen to be the result of scattering on the migrated section.

2. Observation: Some of the dipping events show amplitude increases as travel time increases (2 on fig. 3a).

   Interpretation: Local, high amplitude anomalies are probably overcompensated attenuation correction, constructive interference, or both.

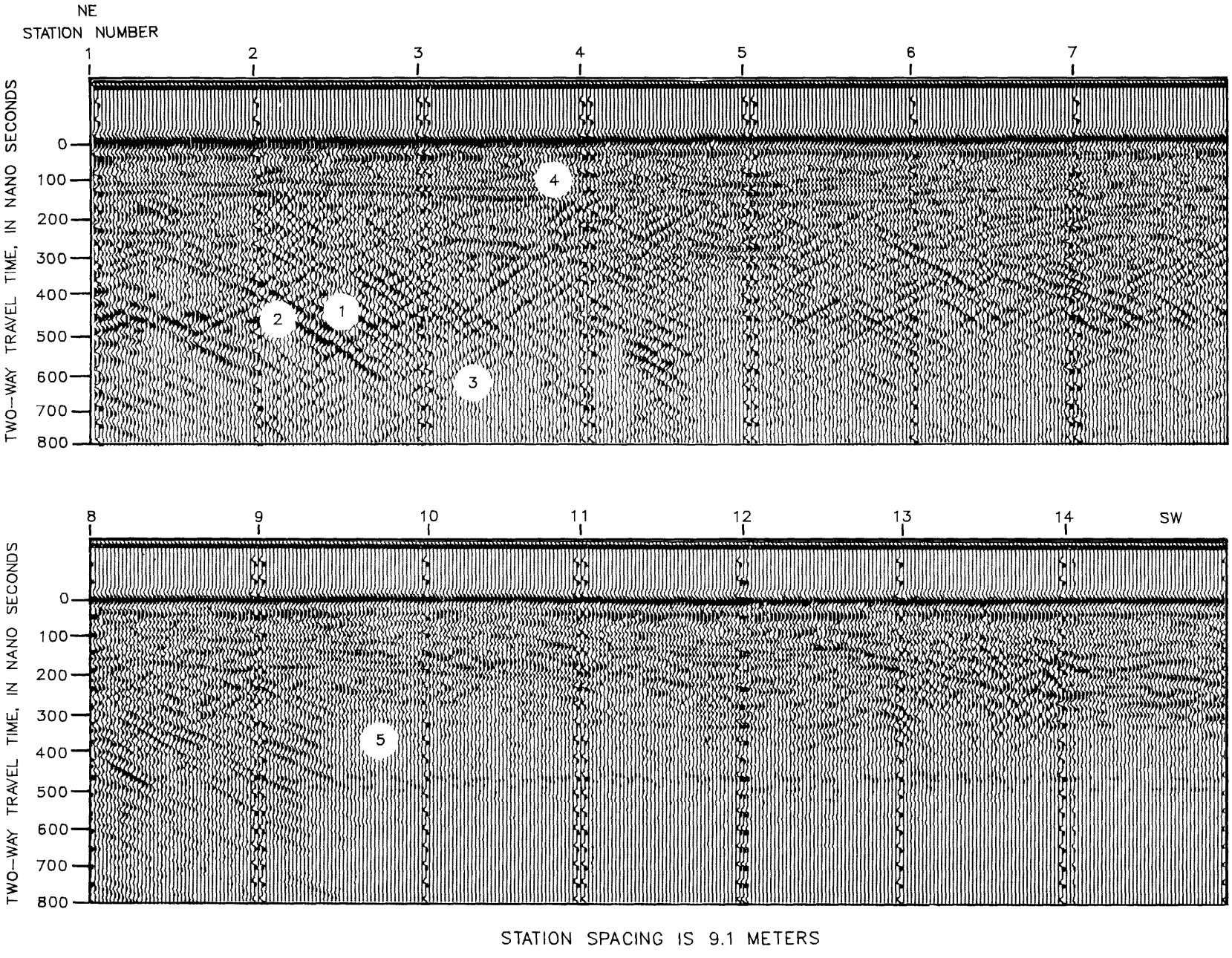

Figure 3.--Northeast-southwest ground-probing radar section.
(a) unmigrated; numbers referred to in text

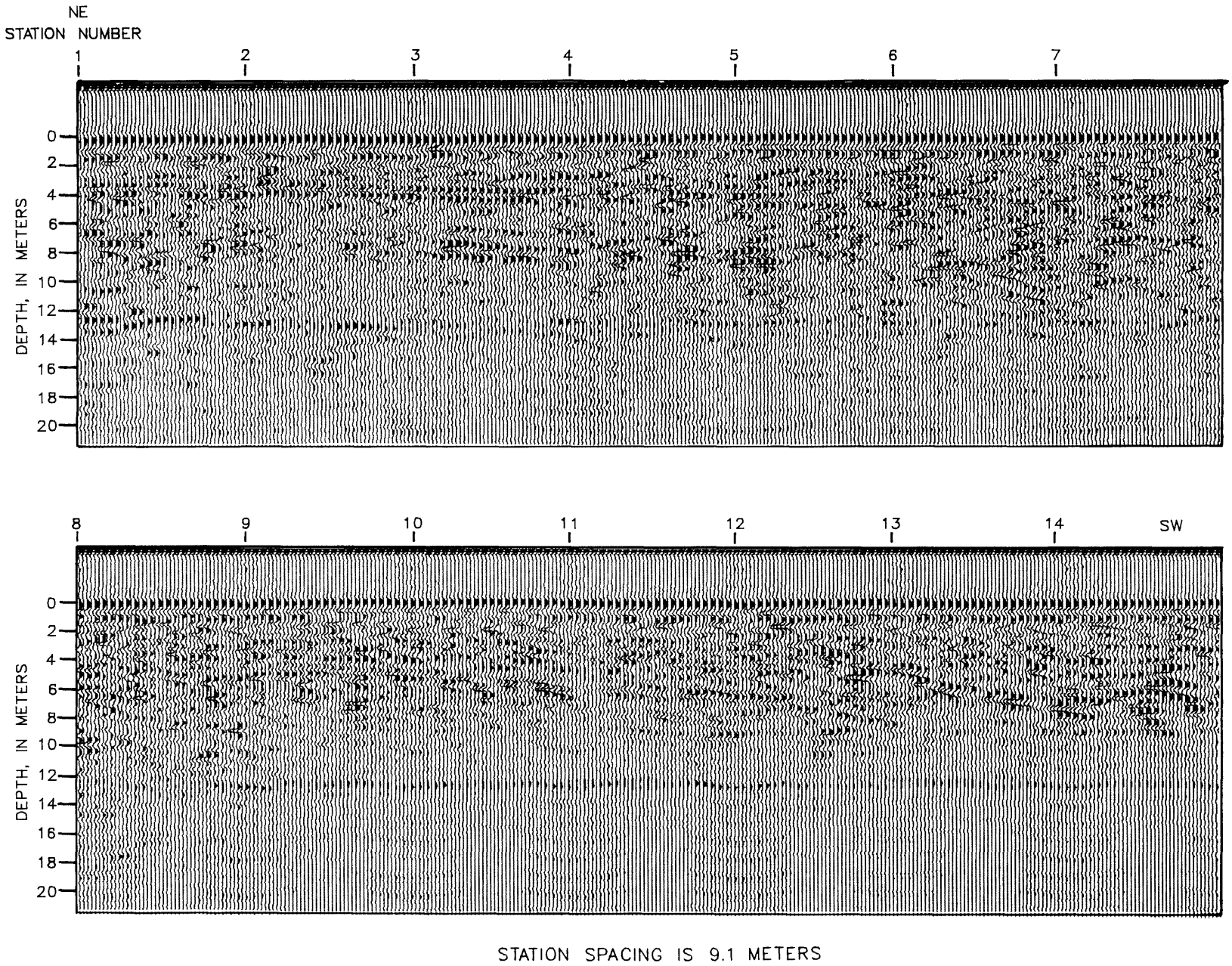

Figure 3.--Northeast-southwest ground-probing radar section.--continued
(b) migrated with velocity equal to 0.057 meters per nanosecond.

3. Observation: Events can be seen down to at least 600 ns and perhaps as far as the complete range of 800 ns (two-way travel time) (3 on fig. 3a). The range over which events occur is decreased to about 350 ns after migration (fig. 3b).

   Interpretation: The interaction of strong subsurface scattering with overcompensated gain correction gives the appearance of greater penetration on the unmigrated record.

4. Observation: Subhorizontal events are present. The subhorizontal event at about 100 ns (about 2.7 m on the migrated section), between stations 1 and 7, appears to truncate all the dipping events (4 on fig. 3a).

   Interpretation: A significant amount of scattering occurs below the top of bedrock, possibly because of discontinuous subhorizontal layering as indicated in the migrated section (fig. 3b). The event at about 2.7 m (fig. 3b) is interpreted as the top of the bedrock. The event at 8.3 m (fig. 3b) is an artifact caused by instrument noise. The event at about 5.4 m may be a multiple reflection of the top of the bedrock. Alternatively, it may be foliation in a massive rock, foliation with superimposed fractures, or fractures in an unfoliated rock.

5. Observation: There is a marked change in attenuation along the section (5 on fig. 3a).

   Interpretation: The increased attenuation along the line coincides with a change from an old logging road to an improved dirt road. The fill used to construct the dirt road has a higher conductivity than that of the natural material on the logging road as a result of either increased water saturation, clay minerals, or both.

Inductive Terrain Conductivity

Inductive terrain-conductivity data were collected using the EM-34--a Slingram type dual-loop instrument manufactured by Geonics Inc. Both horizontal and vertical dipole data were collected along a line oriented NNE. A station spacing of 3.0 m and a coil separation of 20 m was used along the line. The line was offset where the logging road jogged, and the coil separation was parallel to the line. Field measurements could be read to $\pm$0.2 mS/m or better. Where unstable readings were obtained, multiple readings were made and, if necessary, stations were reoccupied at later times.

Contributions to the noise included soil moisture variations (W.M. Kappel, U.S. Geological Survey, written commun., 1990), manmade interference, and atmospheric effects, which could generally be eliminated because of the obvious long period drift in the meter readings at a given station.

Observation and Interpretation

Observation: The vertical-dipole data are fairly uniform except for a single positive anomaly centered 91 m (fig. 4) from the beginning of the line. The maximum anomaly is 0.7 mS/m higher than the surrounding values.

Interpretation: The polarity of the anomaly is opposite to that of a thin vertical conductor and exhibits a shorter than expected wavelength. Considering that the data values are near the instrument's detection limit, the anomaly is interpreted as an artifact produced by noise.

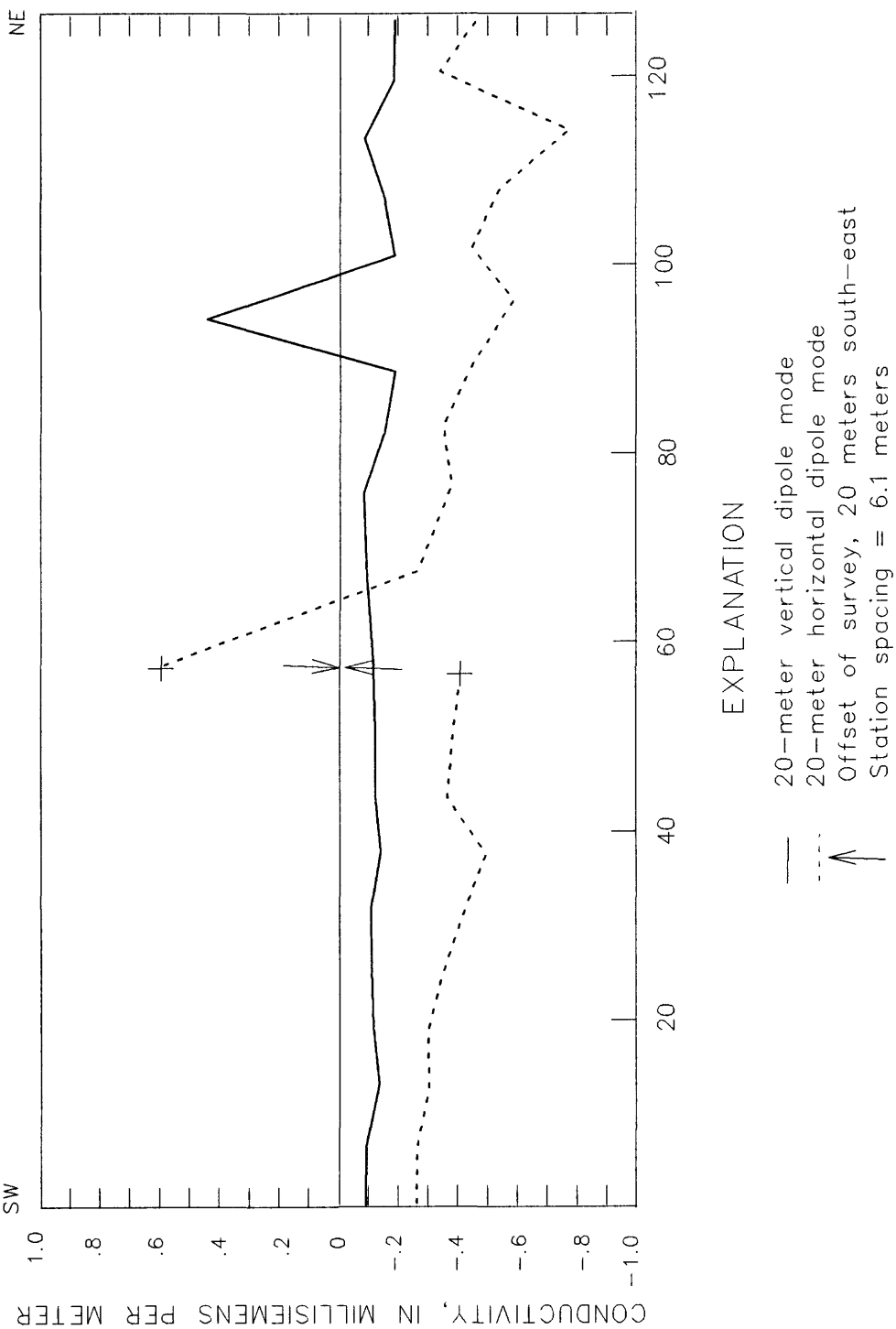

Figure 4.--Plot of inductive terrain-conductivity data.

Direct-Current Resistivity

Data were collected in a standard Schlumberger array: A pair of current electrodes enclose a pair of voltage electrodes located on the same line and with a common center point. The current electrode spacing (AB) is large compared to the voltage electrode spacing (MN) and is progressively enlarged while the voltage electrode spacing is increased only to maintain a measurable potential. Soundings for AB/2 from 3 m to 80 m and MN/2 from 0.5 to 4 m were collected with the Bison 2390 earth resistivity instrument. The soundings were spaced 22.5° apart in azimuth. Plots of smoothed but unshifted apparent resistivities as a function of azimuth for each current electrode spacing are shown in figures 5 to 10. The anisotropy quotient, defined here as the ratio of the maximum to the minimum apparent resistivity, is given as a measure of the maximum departure from an isotropic earth.

Noise contributions to the data included telluric currents (the effects of which are reduced significantly by a current reversal and stacking procedure performed in the instrument) and local near-surface resistivity variations near either the current or the voltage electrodes, or both.

The criteria used to determine the most significant orientation at a given AB/2 and MN/2 included a measure of significance and, where applicable, a measure of precision. For a given AB/2 and MN/2 spacing, an average apparent resistivity was calculated from all azimuthal measurements. The significance of a given orientation was determined by calculating its deviation from this average value. The most significant orientation, at a given AB/2 and MN/2 spacing, is defined as the orientation with maximum deviation from the average value. It is particularly important when the maximum and minimum resistivities are not separated by 90°. In addition, for AB/2 with two MN/2 spacings, precision was measured by the magnitude of the change in apparent resistivity between voltage-electrode spacings, for a given azimuth, at a given AB/2, as compared to the average change over all azimuths.

Observations and Interpretations

It is assumed that the complex patterns displayed in the azimuthal plots are significant, and the contributions from causes other than subsurface fractures are small. Despite this, the interpretation procedure was simplified by focusing on the most significant (as defined above) orientation at each AB/2, thereby reducing the complexity. The orientations of lower significance, which show up consistently, are also noted.

Other factors which may contribute to the observed azimuthal variation of resistivity include: resistivity variations near the current and (or) voltage electrodes, telluric currents, the departure of the subsurface from horizontal homogeneous plane layering (foliation), and resistivity inhomogeneities in bedrock other than fractures.

1. Observation: Plots of the apparent resistivities as a function of azimuth (polar plot) and for different current electrode spacings display very complex patterns rather than simple ellipses.

   Interpretation: The data require more than one fracture set. Two interpretations of the complex azimuthal patterns are possible:

a. The polar plots represent simple interference composites in which the directions of the azimuthal resistivity maxima correspond directly to fracture orientations.

b. The polar plots represent complex interference composites which bear no simple direct relation to the orientations of subsurface fractures, but are related to the most electrically conductive pathways through the rock. If this is the case, no simple interpretation is available at this time. Important properties of single or multiple fracture sets that control the resulting azimuthal resistivity variation are orientation, density, saturation, mean length, and depth range.

2. Observation: At AB/2 of 3 m, a NW-orientation is the most significant, as indicated by the minimum, based on the above criteria. Other possible orientations include NNW and east.

   Interpretation: The lack of orthogonality between the maximum and the minimum indicates that a single fracture set orientation is insufficient to explain the data. The complexity of the plot may be the result of interference between a shallow northeasterly directed till anisotropy indicated by the northwest-trending minimum apparent resistivity, and a deeper east and still deeper NNW-oriented bedrock-fracture anisotropy.

3. Observation: For AB/2 spacings of 4 and 5 m, an east orientation, indicated by the maxima, is the most significant, based on the criteria above. It should be noted that the absolute maxima and minima indicated in the figures sometimes differ from those used to determine the significant orientation; if the change in apparent resistivity from one voltage electrode spacing to another, for a given AB/2, deviates significantly from the average change, a voltage electrode anomaly is assumed to be present and a correction is applied. Other possible orientations are NE and NNW.

   Interpretation: An east-trending fracture set is present in the shallow bedrock. The NE- and NNW-trending orientations may reflect contributions from the overlying till and underlying bedrock, respectively.

4. Observation: For AB/2 spacings of 6, 8, 10, 14, 20, 30, 40, 60, and 80 m, the NNW orientation, indicated by the maxima, dominates, based on the same criteria as in 3 above. Other possible orientations include: east to ESE, which is the most significant at some current electrode spacings and is indicated by secondary or tertiary extrema at other current electrode spacings; and NE, which is indicated by secondary and tertiary extrema at some current electrode spacings. The 40-m current-electrode spacing indicates orientations of NNE and east and the 60-m current- electrode spacing indicates a north orientation. The measure of precision for the 40 m AB/2 is low.

   Interpretation: A fracture set trending NNW is present in the deeper bedrock. Other fracture set oriented east to ESE and NE may be present or these orientations may represent the contributions from the overlying material. The ESE orientation may represent a rotation of the interpreted shallower east-striking fracture set with depth, or a separate set. The changes in orientation indicated by the 40 and 60 AB/2 spacings are anomalous with respect to the orientations at smaller AB/2 and at larger (80 m) AB/2. It is therefore unlikely that they represent changes caused by fracturing.

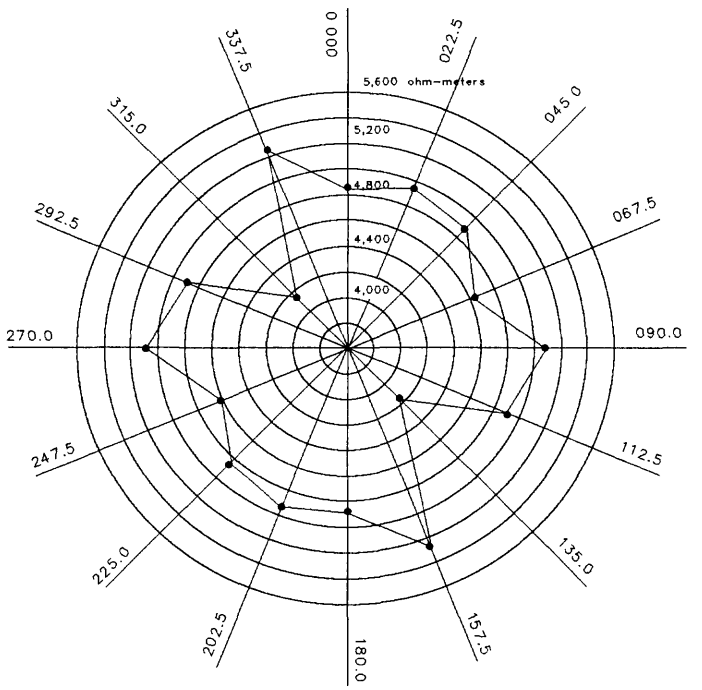

AB/2 = 3 Meters

EXPLANATION

● Apparent resistivity in ohm-meters

——— MN/2 = 0.5 meters

000.0 = Degrees from magnetic north

Anisotropy quotient

MN/2 = 0.5 meters: 5,258/4,160 = 1.26

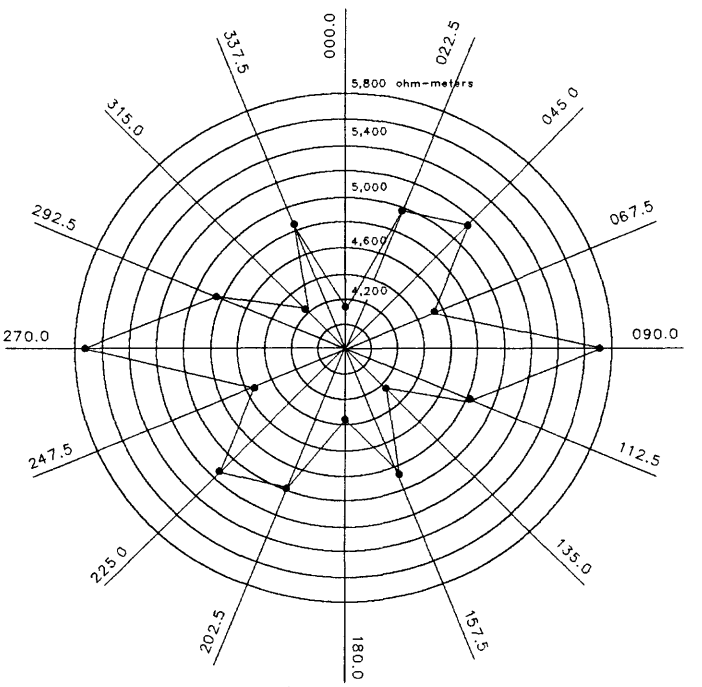

AB/2 = 4 Meters

EXPLANATION

● Apparent resistivity in ohm-meters

——— MN/2 = 0.5 meters

000.0 = Degrees from magnetic north

Anisotropy quotient

MN/2 = 0.5 meters: 5,727/4,158 = 1.38

Figure 5.--Azimuthal plots of apparent resistivity for half-current electrode spacings of 3 and 4 meters.

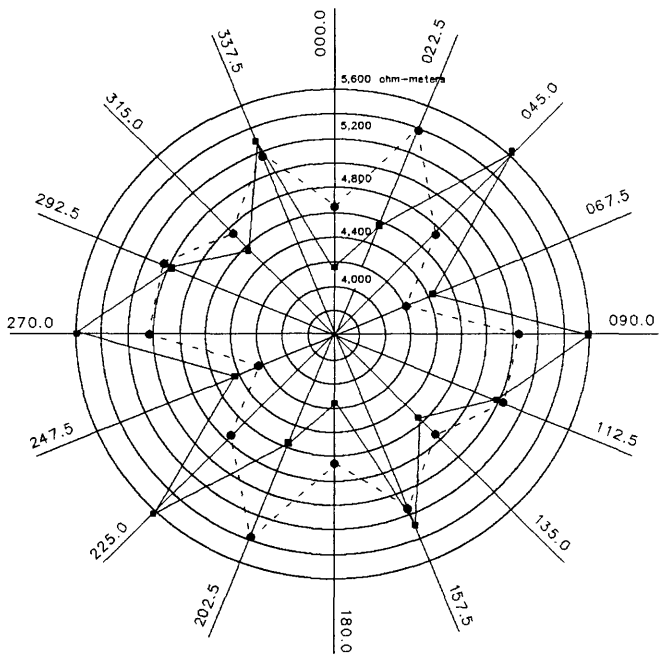

AB/2 = 5 meters

EXPLANATION

• Apparent resistivity in ohm-meters
——— MN/2 = 0.5 meters
- - - - - MN/2 = 1 meter
000.0 = Degrees from magnetic north

Anisotropy quotient

MN/2 = 0.5 meters: 5,621/4,113 = 1.37
MN/2 = 1 meter: 5,399/4,200 = 1.14

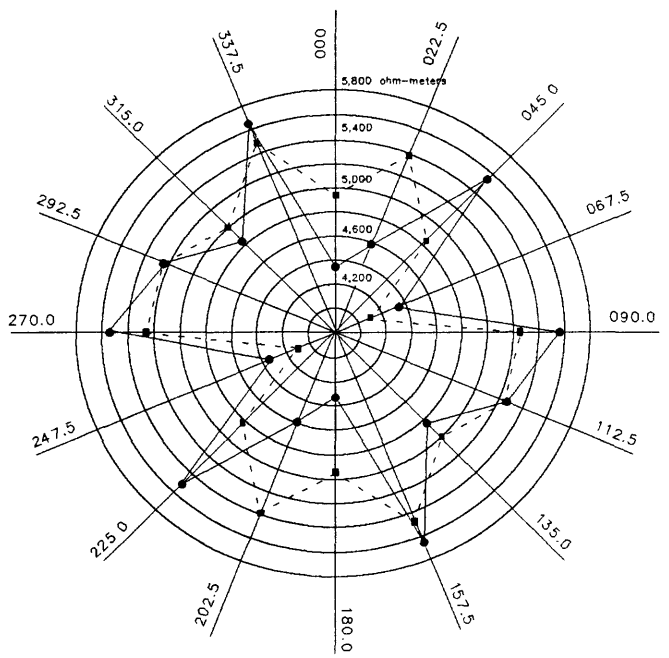

AB/2 = 6 meters

EXPLANATION

• Apparent resistivity in ohm-meters
——— MN/2 = 0.5 meters
- - - - - MN/2 = 1 meter
000.0 = Degrees from magnetic north

Anisotropy quotient

MN/2 = 0.5 meters: 5,659/4,301 = 1.32
MN/2 = 1 meter: 5,489/4,097 = 1.34

Figure 6.--Azimuthal plots of apparent resistivity for half-current electrode spacings of 5 and 6 meters.

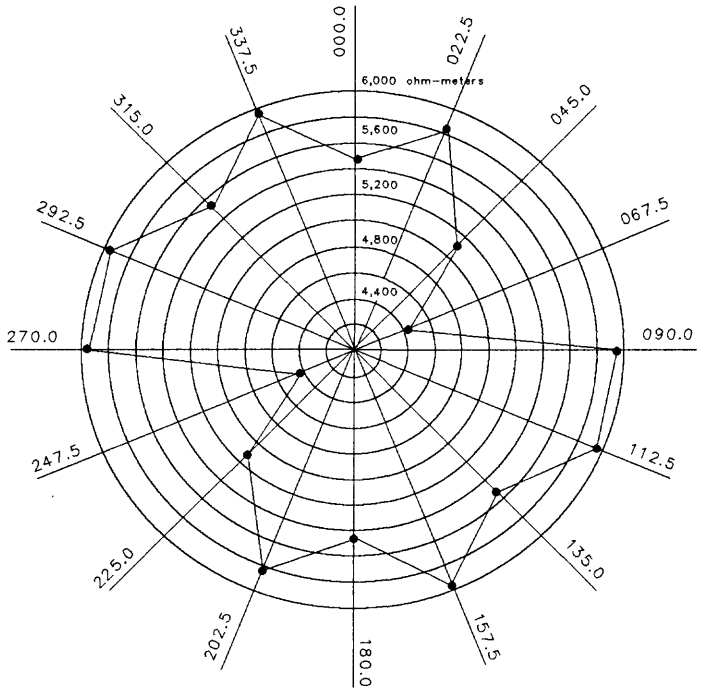

AB/2 = 8 meters

EXPLANATION

• Apparent resistivity in ohm-meters

——— MN/2 = 1 meter

000.0 = Degrees from magnetic north

Anisotropy quotient

MN/2 = 1 meter: 5,970/4,415 = 1.35

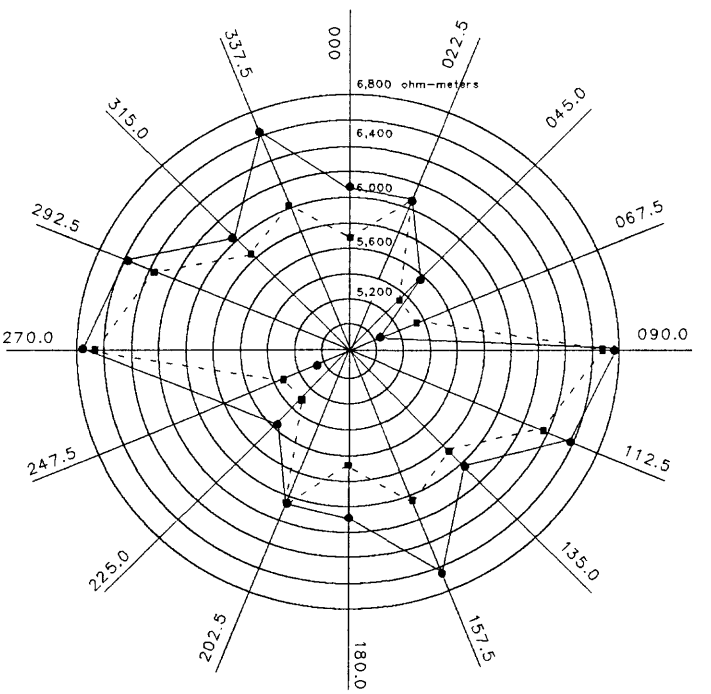

AB/2 = 10 meters

EXPLANATION

• Apparent resistivity in ohm-meters

——— MN/2 = 1 meter

- - - - MN/2 = 2 meters

000.0 = Degrees from magnetic north

Anisotropy quotient

MN/2 = 1 meter: 6,780/5,069 = 1.34

MN/2 = 2 meters: 6,688/5,353 = 1.25

Figure 7.--Azimuthal plots of apparent resistivity for half-current electrode spacings of 8 and 10 meters.

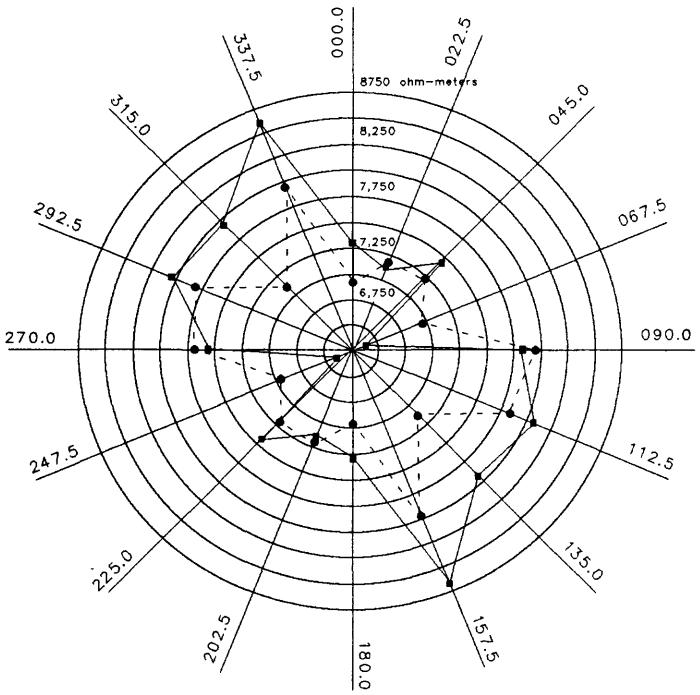

AB/2 = 14 meters

EXPLANATION

• Apparent resistivity in ohm-meters
——— = MN/2 = 1 meter
- - - - = MN/2 = 2 meters
000.0 = Degrees from magnetic north

Anisotropy quotient

MN/2 = 1 meter: 8,668/6,585 = 1.32
MN/2 = 2 meters: 7,796/6,907 = 1.13

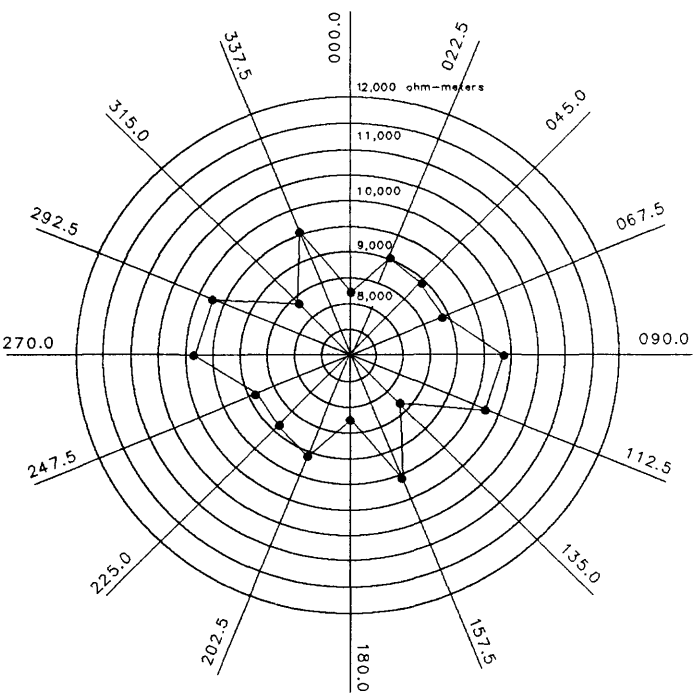

AB/2 = 20 meters

EXPLANATION

• Apparent resistivity in ohm-meters
——— = MN/2 = 2 meters
000.0 = Degrees from magnetic north

Anisotropy quotient

MN/2 = 2 meters: 9,700/8,242 = 1.18

Figure 8.--Azimuthal plots of apparent resistivity for half-current electrode spacings of 14 and 20 meters.

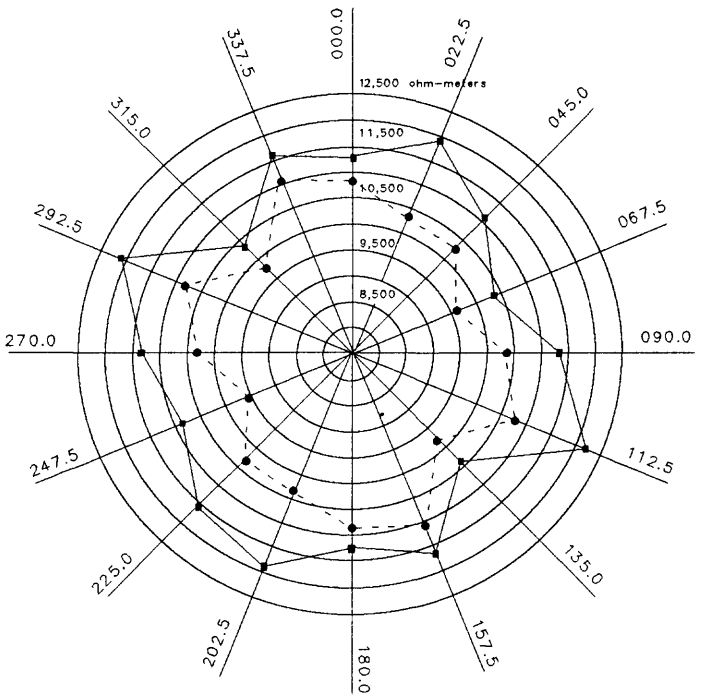

AB/2 = 30 meters

EXPLANATION

• Apparent resistivity in ohm-meters

——— = MN/2 = 2 meters

- - - - - - = MN/2 = 4 meters

000.0 = Degrees from magnetic north

Anisotropy quotient

MN/2 = 2 meters: 12,174/10,415 = 1.17

MN/2 = 4 meters: 11,072/9,615 = 1.15

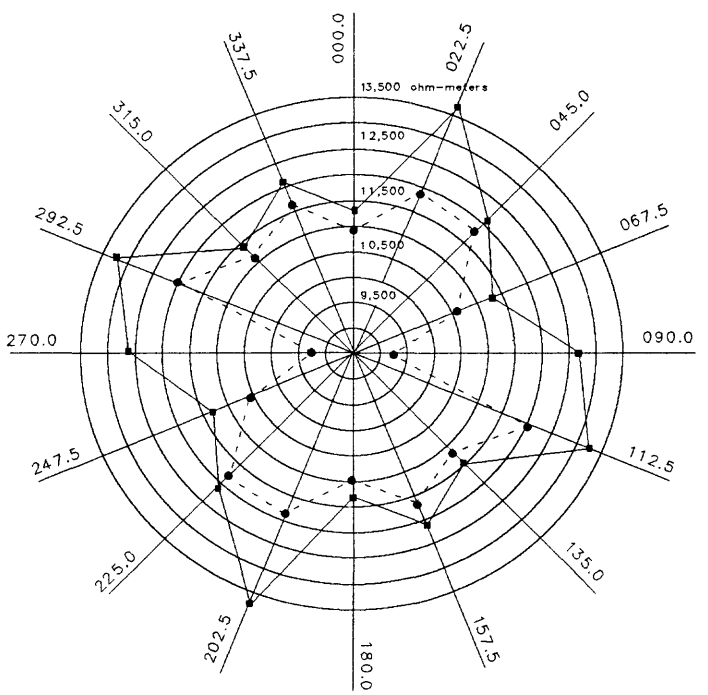

AB/2 = 40 meters

EXPLANATION

• Apparent resistivity in ohm-meters

——— = MN/2 = 2 meters

- - - - - - = MN/2 = 4 meters

000.0 = Degrees from magnetic north

Anisotropy quotient

MN/2 = 2 meters: 13,663/11,267 = 1.21

MN/2 = 4 meters: 12,005/8,956 = 1.34

Figure 9.--Azimuthal plots of apparent resistivity for half-current electrode spacings of 30 and 40 meters.

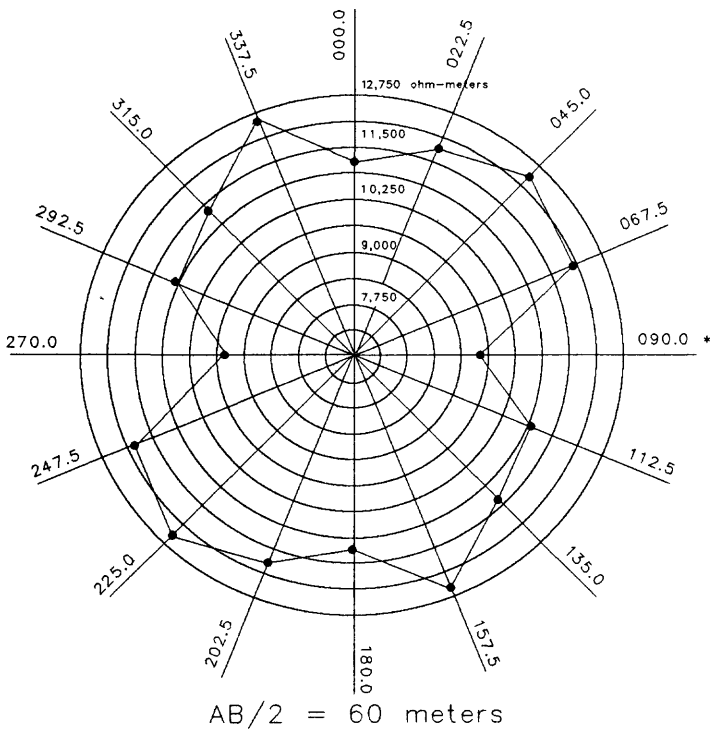

EXPLANATION

• Apparent resistivity in ohm-meters

——— = MN/2 = 4 meters

000.0 = Degrees from magnetic north

Anisotropy quotient

MN/2 = 4 meters: 12,667/9,535 = 1.33

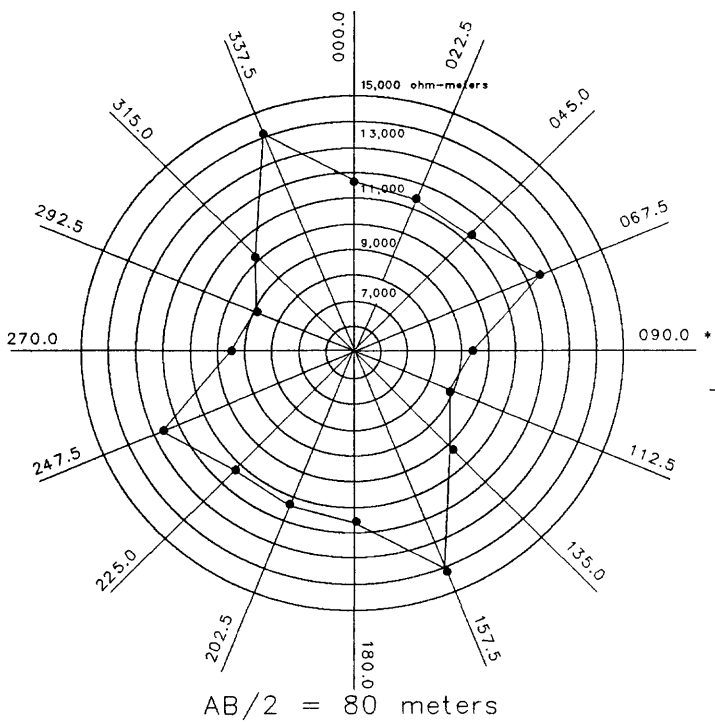

EXPLANATION

• Apparent resistivity in ohm-meters

——— = MN/2 = 4 meters

000.0 = Degrees from magnetic north

Anisotropy quotient

MN/2 = 4 meters: 14,184/8,900 = 1.59

Figure 10.--Azimuthal plots of apparent resistivity for half-current electrode spacings of 60 and 80 meters.

5. Observation: The anisotropy quotient is 1.1 to 1.6.

   Interpretation: The values of anisotropy, obtained here, compare well to the tabulated results of studies from other sites (Risk, 1975; McDowell, 1979; Palacky and others, 1981; Soonawala and Dence, 1981; Taylor, 1982; Mallik and others, 1983; Leonard-Mayer, 1984a, 1984b; Ogden and Eddy, 1984; Taylor, 1984; Taylor and Fleming, 1988).

6. Observation: At AB/2 spacings where azimuthal measurements were obtained for each of two MN/2 spacings, the azimuthal plots sometimes cross.

   Interpretation: The difference between the apparent resistivity values on a given line, obtained for the same current-electrode spacing and two different voltage-electrode spacings, is related to the precision of the measurement and the effects of local subsurface inhomogeneities near the voltage electrodes. Where the change on a given line is close to the average change, the effect of local inhomogeneities is likely to be small. However, the variation of local inhomogeneities from line to line (azimuth to azimuth) may still be the dominant contribution to the observed crossing of the two azimuthal plots obtained at different voltage-electrode spacings. Alternatively, the measurement precision may be the dominant cause of this crossing.

Seismic Refraction

Seismic-refraction data using p-waves were acquired by rotating the line in 45° increments about a common center point. For each line, a dynamite charge buried approximately 0.6 m beneath the surface served as the energy source at each shot location. Twelve vertical-displacement geophones were used as receivers. The geophones were spaced 6.1 m apart and there were five shots per line. All lines were reversed. The near end-shot was 3.0 m from the end of the geophone line and the far end-shot was 35.1 m from the end of the geophone line; a center shot increased the coverage of the water table. An EG&G 1210F signal-enhancement seismograph was used to record the data. Elevations were recorded for each shot location and each geophone position to within 0.03 m. Source depths also were recorded.

The presence of dense vegetation diminished the quality of the data by enhancing the ambient noise vibrations caused by wind and low-flying aircraft. Also, topographic relief of about 6 m was present in some directions.

Unlike some of the other geophysical methods used in this study, plots of refraction field data do not easily convey information on p-wave velocity; analysis and interpretation must be performed prior to obtaining p-wave velocity, for a given line direction. Because the interpretation of fracture orientations may change depending on the results of the velocity analysis, the observation section contains a comparison of results obtained from a number of different interpretation methods. The results are presented as azimuthal velocity plots where each value is the result of a velocity analysis on the appropriately oriented refraction line. The different methods of velocity analysis are the linear regression method as implemented in the SIPT program (Haeni and others, 1987) and developed by Scott and others (1972) (fig. 11); the Hobson-Overton (HO) method as implemented in the SIPT program (Haeni and others, 1987) and developed by Scott and others (1972) (fig. 12); and the generalized reciprocal method (GRM) for XY=0, as implemented by Stoyer (1987) and discussed in Palmer (1980) (fig. 13). The value of XY corresponds to the surface distance

between the two rays emerging from the same refractor point and travelling towards opposite ends of the line. The XY value is important in velocity analysis and depth conversion.

Note that the use of the GRM in this report is an approximation. The GRM requires the measurement of reciprocal times and these surveys were not designed for the GRM; therefore, reciprocal times were linearly extrapolated from the measured data. Because velocity analysis is relatively insensitive to reciprocal time, this is not a problem. However, the results of depth conversion are sensitive to reciprocal time, and therefore no depth converted sections were produced based on the extrapolated data. The observations are presented below.

Observations and Interpretations

Where the absolute maximum and minimum are not orthogonal, the maximum deviation from the average velocity was used to identify the most significant orientation.

Fracturing of the bedrock is assumed to be the primary cause of the complexity of the azimuthal plots. Other factors which may contribute to the observed azimuthal variation of p-wave velocities include lateral variation of the p-wave velocity and the thickness of the first (overburden) layer and p-wave velocity inhomogeneities other than fractures within the bedrock.

The simplest interpretation of the velocity data uses the linear-regression method. This method makes a best-fit straight line through the arrival times from a designated layer. Large scale variation in overburden thickness can be accounted for but was neglected in this implementation, inasmuch as the velocities obtained from opposing shots were averaged. Thickness changes and lateral variations in velocities that occur on scales small compared to the line are not accounted for. The HO method (Scott and others, 1972; Scott, 1973) uses linear regression but applies it to delay time--a quantity that incorporates the reversed shots explicitly and is, therefore, a more refined method for calculating the velocity than simple regression.

Velocity analysis using the GRM method where XY=0 is reported to be similar to that using the HO method (Palmer, 1980, p. 7). The optimum GRM utilizes an optimum value of XY. (Optimum XY is the distance between surface geophones where refracted rays from reversed shots emerge from the same point on the refractor.) This method requires the field aquisition of reciprocal times, which could only be estimated in this study. In theory, the optimum GRM is the method least sensitive to velocity and thickness changes in the overburden and to change in the seismic velocity of the refractor. A comparison of the different methods of seismic-refraction data interpretations is given by Scott and Markiewicz (1990).

1. Observation: The most significant orientation, obtained from the linear regression interpretation of p-wave velocities (fig. 11) is NE.

   Interpretation: A fracture set trending NE is interpreted from the linear regression method of velocity analysis (fig. 11).

2. Observation: The east orientation, indicated by the maximum, is the most significant orientation indicated by the HO method of velocity analysis (fig. 12).

Interpretation: An east-trending fracture set is interpreted from the HO method of velocity analysis (fig. 12). Alternatively, the NW velocity minimum can be interpreted as being perpendicular to the trend of a fracture set trending NE.

3. Observation: The east orientation, indicated by the maximum, is the most significant orientation indicated by the GRM of velocity analysis, for XY=0 (fig. 13). XY=0 also corresponds to the optimum XY at this site.

   Interpretation: An east-trending fracture set is interpreted from the GRM of velocity analysis (fig. 13). Alternatively, the NW velocity minimum can be interpreted as being perpendicular to the trend of a fracture set oriented NE. The optimum XY (=0) implies that bedrock is near the surface; this is supported by the SIPT depth interpretations that show bedrock to be less than about 3 m below the surface over most of the area.

4. Observation: The velocities obtained by the regression method are uniformly lower than those obtained by either GRM or HO.

   Interpretation: Refractor topography as well as variations in overburden velocity, which are unaccounted for in the regression method, are the likely contributions to the uniformly lower velocities obtained by the regression method as compared to the HO and GRM methods of velocity analysis.

5. Observation: Although the NW direction, the azimuth of minimum velocity, is consistent between the GRM, HO, and the regression methods, the azimuth of maximum velocity is not. The GRM and HO both yield an east-trending maximum whereas the regression yields a NE-trending maximum. In no case is the azimuthal distribution of velocity a simple ellipse.

   Interpretation: Only one fracture set orientation is interpreted from seismic data because the sparse azimuthal sampling does not constrain the orientation of a second set. For a single set of fractures, the velocity maximum and minimum should be orthogonal; both the HO and GRM (XY=0) show a nonorthogonal maximum and minimum. A lack of data precision, undersampling of a complex azimuthal velocity function, unaccounted for geologic complexity, and (or) a subsurface with more than one fracture set can explain occurrences where the velocity maximum and minimum are not 90° apart. Interpretation of this data in terms of a single east-trending fracture set is based on the east-trending velocity maximum, which is the most significant orientation in both the HO and GRM results, and because these methods are considered more reliable that the regression method. However, the NE orientation, defined consistently by the velocity minima, cannot be ruled out.

6. Observation: The anisotropy quotient, the ratio of the maximum to minimum interpreted azimuthal velocity, obtained from the different methods, is as follows: GRM=1.08; HO=1.05; regression=1.05. The anisotropy quotient is a measure of the deviation from an isotropic earth.

   Interpretation: The magnitude of anisotropy, as expressed by the anisotropy quotient, is comparable to that obtained in other studies (Bamford and Nunn, 1979; Crampin and others, 1980; Park and Simmons, 1982; Imse and Levine, 1985).

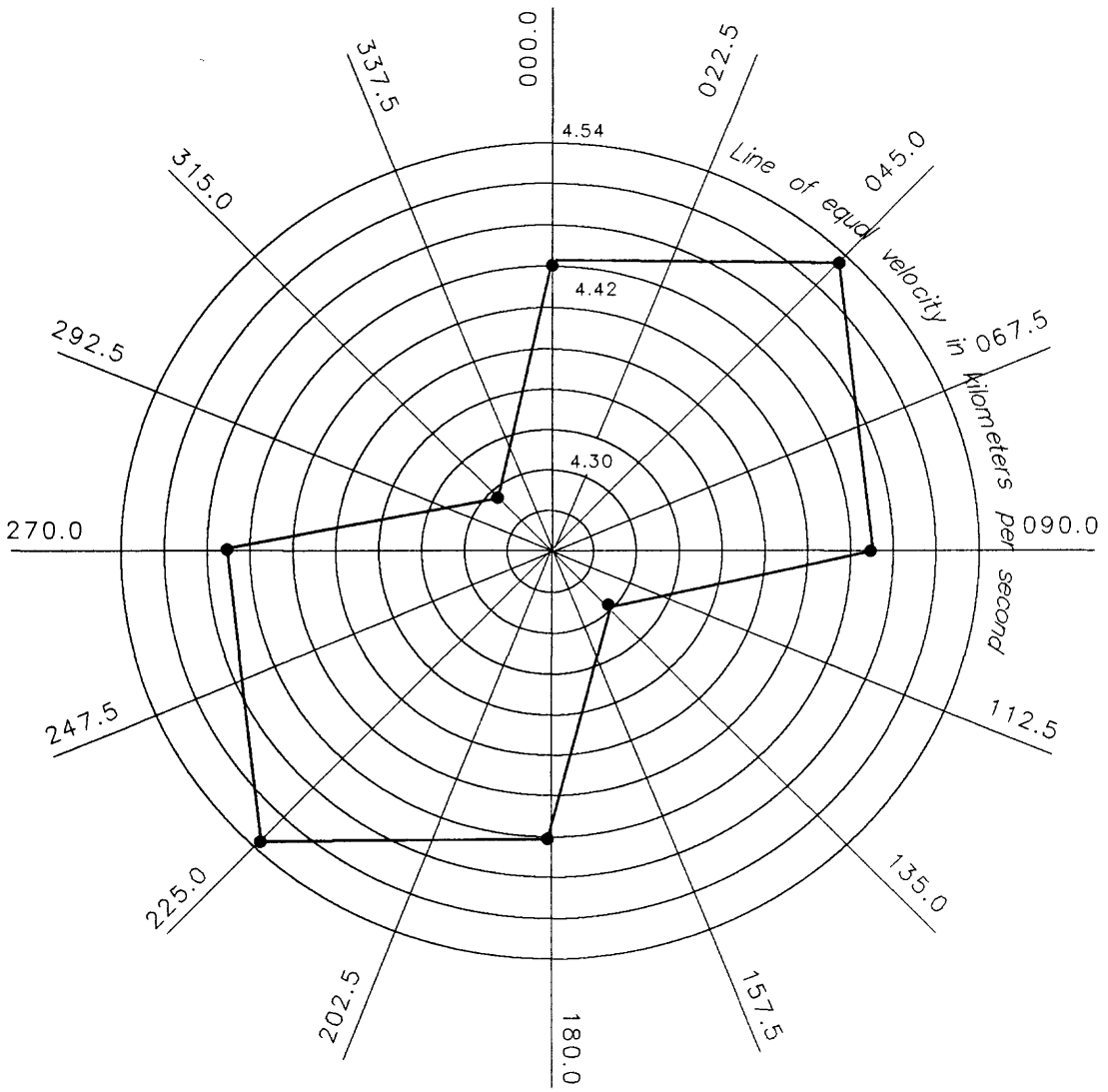

EXPLANATION

● Seismic p-wave velocity in bedrock

000.0 = Degrees from magnetic north

Anisotropy quotient

4.53/4.29 = 1.05

Figure 11.--Azimuthal plot of p-wave velocity in bedrock obtained by the linear-regression method of velocity analysis.

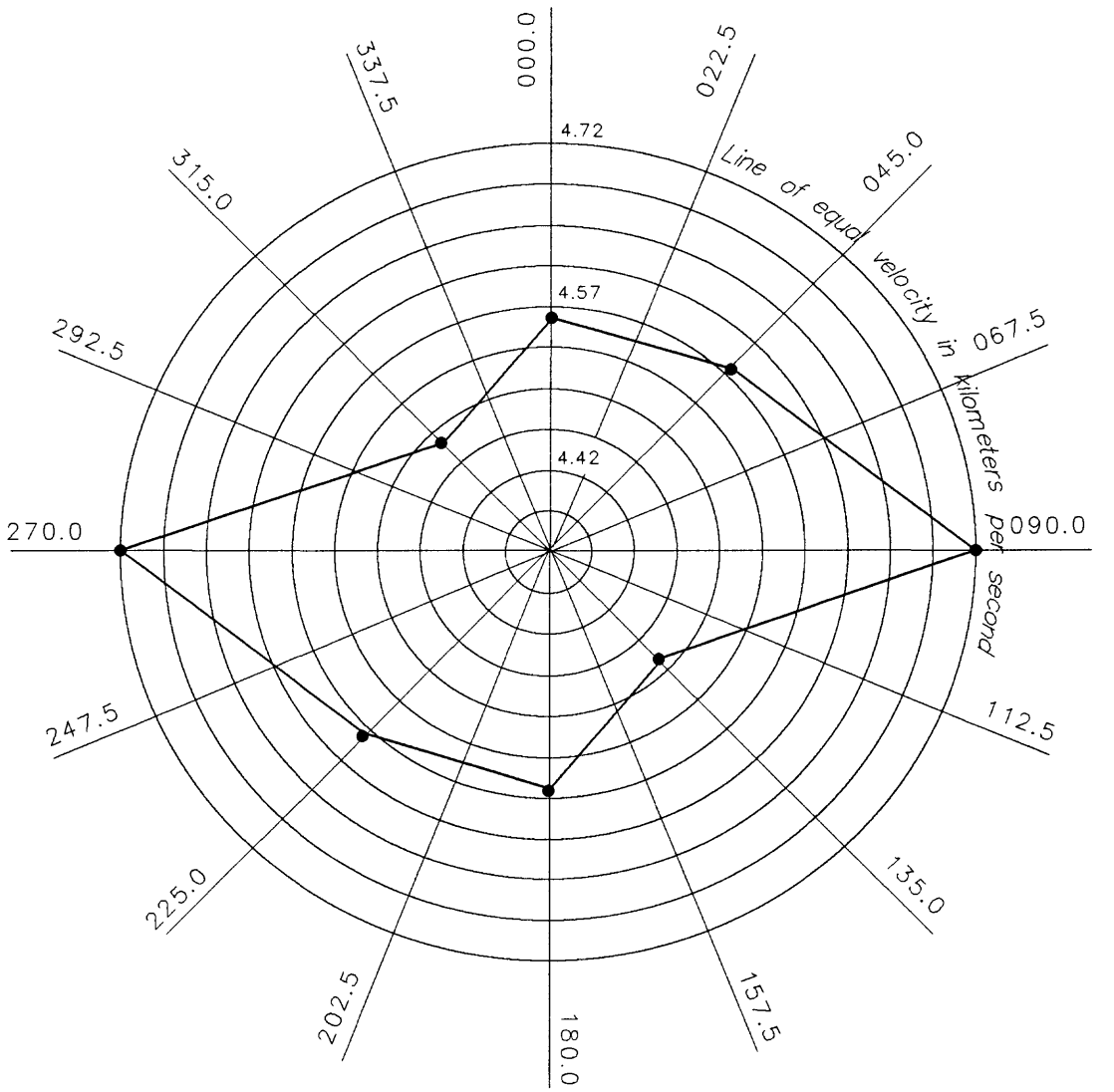

EXPLANATION

● Seismic p-wave velocity in bedrock

000.0 = Degrees from magnetic north

Anisotropy quotient

4.72/4.48 = 1.05

Figure 12.--Azimuthal plot of p-wave velocity in bedrock obtained by the Hobson-Overton method of velocity analysis.

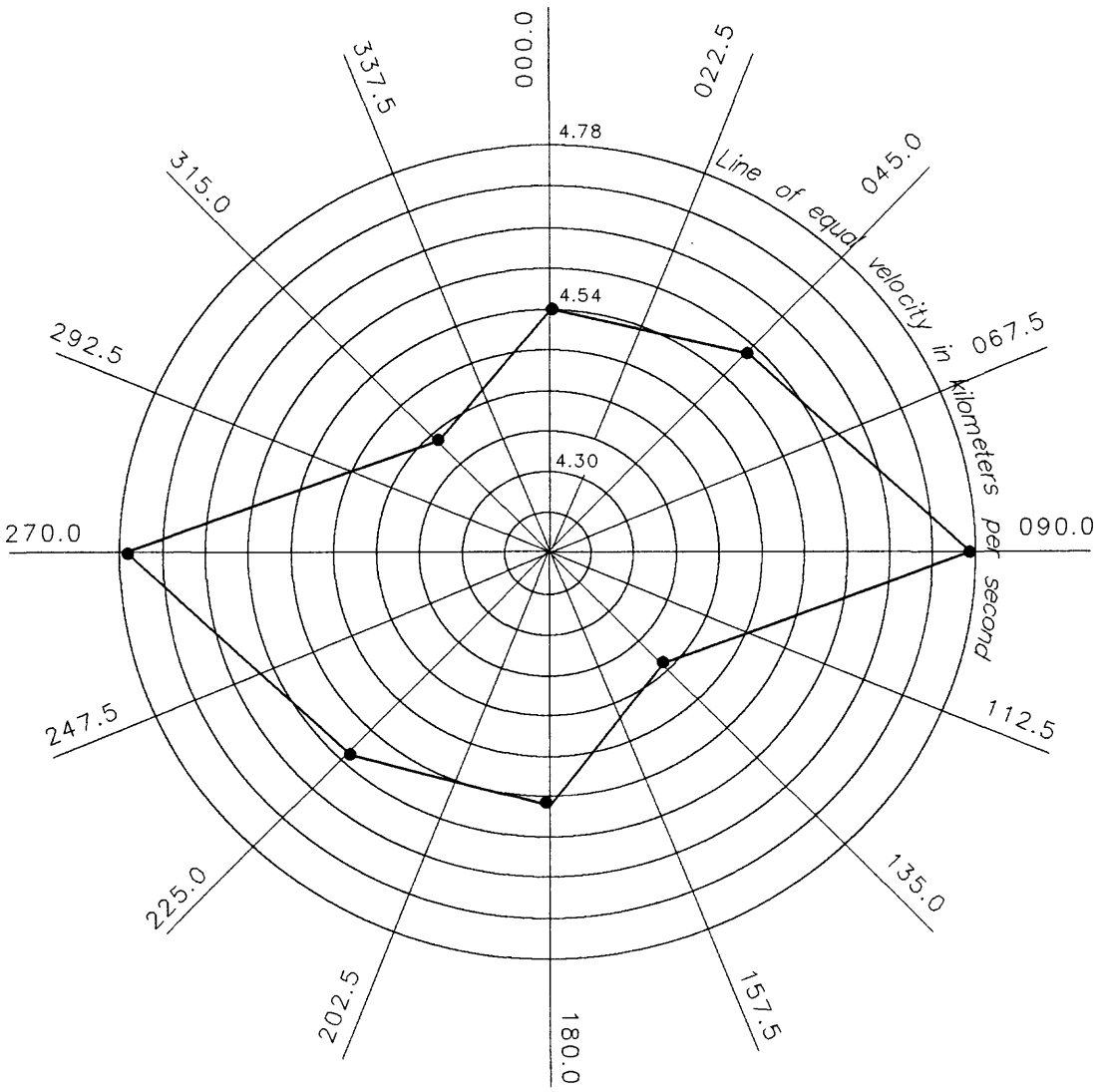

Figure 13.--Azimuthal plot of p-wave velocity in bedrock obtained by the generalized reciprocal method of velocity analysis for XY=0.

CORRELATIONS AMONG GEOPHYSICAL, GEOLOGIC, AND HYDROLOGIC DATA

Correlations Among Geophysical Data

The DC-resistivity data are the most complex of the four data sets. The results of the DC-resistivity interpretation indicate a subsurface containing more fracture sets than the seismic refraction or GPR data sets. This probably reflects the differences in sensitivities of the methods to subsurface fracturing.

DC-resistivity data for AB/2 of 4 and 5 m show a significant easterly orientation. Decimation of the DC-resistivity data for all AB/2, in order to eliminate sampling bias between the DC and seismic data sets, yields an easterly orientation throughout. Because depth to bedrock is approximately 3 m (determined from seismic-refraction and GPR data), the east-trending anomaly present at AB/2 at 4 and 5 m is interpreted to be representative of fractures in the shallow bedrock. An east-trending fracture set is also interpreted from the seismic-refraction data, which is representative of the shallow bedrock. An east-trending fracture set is therefore a reasonable interpretation for both geophysical methods at shallow depths. A NNW-trending fracture set is probably present at greater depths.

The presence of steeply dipping fractures is interpreted from measured anisotropy in both DC-resistivity and seismic-refraction methods. The reflections in the GPR record, however, are from subhorizontal targets. The best correlation between the GPR results and those of the other two methods is that steeply dipping fractures and subhorizontal foliation with or without superposed fractures may be present at this site.

Correlations Among Geophysical, Geologic and Hydrologic Data

Well B6-D, the only well from which a core was collected, encountered a subhorizontal foliation, as well as subhorizontal and steeply dipping fractures (NHWSPCC, 1985). If the subhorizontal foliation can be extrapolated to the survey site, many of the scattering events below the bedrock surface may be attributable to local variation in foliation, with possible superposed fracturing. The steeply dipping fractures observed in the core are not seen in the radar data; however, they may contribute to the anisotropy observed in both the DC-resistivity and seismic-refraction data. Unfortunately, the orientation of the steeply dipping fractures was not obtained from the core.

Hydraulic connections with orientations of ESE to SE and NNW were obtained from aquifer tests. Outcrop data and aerial photographs indicate dominant NW trending fractures with possibly important ENE- and WNW-trending fractures as well. These orientations are considered close to the east and NW trends interpreted here, within the limitations imposed on the quantified correlation of different data sets.

SUMMARY AND CONCLUSIONS

A study integrating four surface-geophysical methods was conducted to indicate the presence and orientations of subsurface fractures at a site on Tibbetts Road, near Barrington, New Hampshire. The methods used were ground-probing radar, inductive terrain conductivity, DC resistivity, and seismic refraction. The heavily wooded area and the ambient noise level limited the scope of data collection and the quality of the data collected.

The unmigrated GPR line oriented NE has many events that dip towards the SW and NE. Others that are subhorizontal and less pervasive are also present. After migration, the dipping events disappear and are thus attributed to scattering. The shallowest (about 3 m) event is the bedrock surface. At 6 m, an event that is probably a multiple reflection of the bedrock surface occurs, and an event just below about 8 m is an artifact caused by instrument noise. Strong scattering that occurs below the bedrock surface may reflect variations caused by foliation with possible superposed fracturing. No anomalies that could be interpreted as being caused by fractures or fracture zones were present in the single line of inductive terrain-conductivity data.

Azimuthal anisotropy is present in the DC-resistivity data sets. This anisotropy is interpreted as being indicative of two sets of subsurface fractures trending east and NNW. Alternatively, these trends may be interference composites. In this case, the orientation(s) of the maxima would bear little relation to the actual trend(s) of fractures; however, these maxima would still be related to the most electrically conductive pathways through the rock and therefore may be related to hydraulic properties. An east-trending fracture set is interpreted from the seismic-refraction data alone.

An east-trending fracture set is obtained by correlating the DC-resistivity results with the seismic-refraction results at shallow depths. A NNW-trending fracture set is indicated at deeper depths.

Local fracture trends indicated in this report are close to the trends of hydraulic connections obtained during hydraulic testing and to the trends of fractures and fracture zones in regional geologic outcrop data and aerial photographs. The amount of available data limit the degree to which these different data sets can be said to match one another.

Existing methods of data collection, analysis, and interpretation should be used with caution when they are applied to problems involving the detection of subsurface fracturing. More theoretical and empirical work is required to understand (a) the use of the different methods in fractured rock, (b) the effects of nongeologic noise on the data and its interpretation, (c) the effects of assumptions associated with each geophysical method in the analysis and interpretation, and (d) the degree to which the correlation of multiple data sets can restrict the number of possible subsurface geologic interpretations, even if some individual methods fail to detect anomalies attributable to fractures.

REFERENCES

Bamford, David, and Nunn, K.R., 1979, In-situ seismic measurements of crack anisotropy in the Carboniferous limestone of northwest England: Geophysical Prospecting, v. 27, p. 322-338.

BCI Geonetics, Inc, 1984, Bedrock fracture fabric analyses of the Tibbetts Road site, Barrington, N.H.- Hydrogeologic support investigation for New Hampshire Water Supply and Pollution Control Commission: Laconia, New Hampshire, BCI Geonetics, 15 p.

Crampin, Stuart, McGonigle, Robert, and Bamford, David, 1980, Estimating crack parameters from observations of P-wave velocity anisotropy: Geophysics, v. 45, no. 3, p. 345-360.

Frazer, L.N., 1990, Dynamic elasticity of microbedded and fractured rocks: Journal of Geophysical Research, v. 95, no. B4, p. 4821-4831.

Haeni, F.P., Grantham, D.G., and Ellefsen, Karl, 1987, Microcomputer-based version of SIPT--A program for the interpretation of seismic-refraction data: U.S. Geological Survey Open-File Report 87-103A (text), 13 p. and 87-103B, 5¼-inch disk, MS-DOS compatible.

Imse, J.P., and Levine, E.N., 1985, Conventional and state of the art geophysical techniques for fracture detection: National Water Well Association Annual Eastern Regional Groundwater Conference, 2nd, Portland, Maine, 1985, Proceedings, p. 18-36.

Keller, G.V., and Frischknecht, F.C., 1966, Electrical methods in geophysical prospecting: Oxford, England, Pergamon Press, 523 p.

Leonard-Mayer, P.J., 1984a, A surface resistivity method for measuring hydrologic characteristics of jointed formations: U.S. Bureau of Mines Report of Investigations 8901, 45 p.

_____ 1984b, Development and use of azimuthal resistivity surveys for jointed formations, in Nielsen, D.M., and Curl, Mary, (eds.), National Water Well Association/U.S. Environmental Protection Agency Conference on Surface and Borehole Geophysical Methods in Ground-Water Investigations, San Antonio, Texas, Proceedings: Worthington, Ohio, National Water Well Association, p. 52-91.

Mallik, S.B., Bhattacharya, D.C., and Nag, S.K., 1983, Behaviour of fractures in hard rocks--A study by surface geology and radial VES method: Geoexploration, v. 21, p. 181-189.

McCormick, M.W., 1989, Site analysis of Tibbetts Road site, Barrington, N.H.: Las Vegas, Nevada, U.S. Environmental Protection Agency Environmental Systems Monitoring Lab, TS-PIC-89021, 17 p.

McDowell, P.W., 1979, Geophysical mapping of water filled fracture zones in rocks: International Association of Engineering Geology Bulletin, v. 19, p. 258-264.

McNeill, J.D., 1980a, Electromagnetic terrain conductivity measurement at low induction numbers: Geonics Limited, Technical Note TN-6, 15 p.

_____ 1980b, EM34-3 survey interpretation techniques: Geonics Limited, Technical Note TN-8, 16 p.

New Hampshire Water Supply and Pollution Control Commission (NHWSPCC), 1985, Hydrological investigation, Tibbetts Road hazardous waste site, Barrington, N.H.: Concord, N.H., Commission Report 144, 173 p.

Ogden, A.E., and Eddy, P.S., Jr., 1984, The use of tri-potential resistivity to locate fractures, faults and caves for siting high yield water wells, in Nielsen, D.M., and Curl, Mary, (eds.), National Water Well Association/U.S. Environmental Protection Agency Conference on Surface and Borehole Geophysical Methods in Ground-Water Investigations, San Antonio, Texas, Proceedings: Worthington, Ohio, National Water Well Association, p. 130-149.

Olsson, Olle, Andersson, P., Carlsten, S., Falk, L., Niva, Borje, and Sandberg, E., 1988, Fracture characterization in crystalline rock by borehole radar: Workshop on Ground Penetrating Radar, May 24-26, Ottawa, Canada, 24 p.

Palacky, G.J., Ritsema, I.L., and De Jong, S.J., 1981, Electromagnetic prospecting for groundwater in Precambrian terrains in the Republic of Upper Volta: Geophysical Prospecting, v. 29, p. 932-955.

Palmer, Derek, 1980, The generalized reciprocal method of seismic interpretation: Tulsa, Oklahoma, Society of Exploration Geophysicists, 104 p.

Park, Stephen, and Simmons, Gene, 1982, Crack induced velocity anisotropy in the White Mountains, New Hampshire: Journal of Geophysical Research, v. 87, no. 84, p. 2977-2983.

Posten, Stephen, Karmazinski, Paul, and Nicholas, Michael, 1986, Geohydrological investigations Tibbetts Road site, Barrington, N.H.-Well installation, well monitoring, estimation of aquifer flow, contaminant migration and hydraulic properties: Washington D.C., U.S. Environmental Protection Agency Environmental Emergency Response Unit, 63 p.

Risk, G.F., 1975, Detection of buried zones of fissured rock in geothermal fields using resistivity anisotropy measurements, in Geophysical papers submitted to the second U.N. symposium on the development and use of geothermal resources: San Francisco, California, 20-29 May, p. 78-100.

Scott, J.H., 1973, Seismic refraction modeling by computer: Geophysics, v. 38, no. 2, p. 271-284.

Scott, J.H., and Markiewicz, R.D., 1990, Dips and chips--PC programs for analyzing seismic refraction data: Symposium on the Application of Geophysics to Engineering and Environmental Problems, Golden, Colorado, Society of Engineering and Mineral Exploration Geophysicists, Proceedings, 25 p.

Scott, J.H., Tibbetts, B.L., and Burdick, R.G., 1972, Computer analysis of seismic refraction data: U.S. Bureau of Mines Report of Investigation 7595, 95 p.

Soonawala, N.M., and Dence, M.R., 1981, Geophysics in the Canadian nuclear waste program--A case history: Society of Exploration Geophysicists Annual International Meeting, 51st, Los Angeles, Calif., 1981, Proceedings, p. 83-98.

Stoyer, C.H., 1987, Gremix: Golden, Colorado, Interpex, Ltd., 127 p.

Taylor, R.W., 1982, Evaluation of geophysical surface methods for measuring hydrological variables in fractured rock units: U.S. Bureau of Mines Research Contract Report, contract H0318044, 147 p.

_____ 1984, The determination of joint orientation and porosity from azimuthal resistivity measurements, in Nielsen, D.M., and Curl, Mary, (eds.), National Water Well Association/U.S. Environmental Protection Agency Conference on Surface and Borehole Geophysical Methods in Ground-Water Investigations, San Antonio, Texas, Proceedings: Worthington, Ohio, National Water Well Association, p. 37-49.

Taylor, R.W., and Fleming, A.H., 1988, Characterizing jointed systems by azimuthal resistivity surveys: Ground Water, v. 26, no. 4, p. 464-474.

Ulriksen, C.P.F., 1982, Application of impulse radar to civil engineering: Hudson, N.H., Geophysical Survey Systems, Inc., 179 p.

van Lissa, R.V., van Maanen, H.R.J., and Odera, F.W., 1987, The use of remote sensing and geophysics for groundwater exploration in Nyanza Province, Kenya: African Water Technology Conference, Nairobi, February 1987, 24 p.

Villegas-Garcia, C.J., and West, G.F., 1983, Recognition of electromagnetic overburden anomalies with horizontal loop electromagnetic survey data: Geophysics, v. 48, no. 1, p. 42-51.

Wait, J.R., 1990, Current flow into a three dimensionally anisotropic conductor: Radio Science, v. 25, no. 5, p. 689-694.

Yager, R.M., and Kappel, W.M., 1988, Detection and characterization of fractures and their relation to ground-water movement in the Lockport Dolomite, Niagara County, New York, in 3rd Annual Groundwater Technology Conference: New York, New York, Proceedings, September 1988, 47 p.

★U.S. GOVERNMENT PRINTING OFFICE: 1992 - 700-337/60036